

# Exact Dynamical Equations for Kinetically-Constrained-Models

Gianmarco Perrupato<sup>1</sup> and Tommaso Rizzo<sup>2,1</sup>

<sup>1</sup>*Dipartimento di Fisica, Sapienza Università di Roma, P.le A. Moro 5, 00185 Rome, Italy*

<sup>2</sup>*Institute of Complex Systems (ISC) - CNR, Rome unit, P.le A. Moro 5, 00185 Rome, Italy*

The mean-field theory of Kinetically-Constrained-Models is developed by considering the Fredrickson-Andersen model on the Bethe lattice. Using certain properties of the dynamics observed in actual numerical experiments we derive asymptotic dynamical equations equal to those of Mode-Coupling-Theory. Analytical predictions obtained for the dynamical exponents are successfully compared with numerical simulations in a wide range of models including the case of generic values of the connectivity and the facilitation, random pinning and fluctuating facilitation. The theory is thus validated for both continuous and discontinuous transition and also in the case of higher order critical points characterized by logarithmic decays.

The question whether glassiness has a thermodynamic origin or it is a purely dynamics phenomenon, the so-called dynamic/structure dilemma, lies at the core of the longstanding debate around the nature of the glass transition [1]. Kinetically-Constrained-Models (KCM) [2, 3] represent an extreme case: they have trivial thermodynamical properties and yet, because of dynamic facilitation, display all the basic features of glassy dynamics. Besides, recent numerical studies [4] performed with the swap technique provide strong evidence that dynamic facilitation is an important ingredient (although it may be not the unique one) for the glassy behavior of supercooled liquids, strengthening earlier insights [5]. Our understanding of KCMs is mainly based on a large body of numerical work covering basically all aspects of their complex dynamics. Important advances have also been made by the mathematical community [3], but from a standard theoretical physics perspective there are essential questions that are still open, and efficient analytical techniques are yet to be developed. One important issue is the connection with Mode-Coupling-Theory (MCT) [6]: efforts to describe theoretically KCM dynamics along this line date back to the very first papers on KCMs [7, 8]. In these earlier analytical treatments, approximations were used to derive MCT-like equations, whose solution displays many non-trivial features of the dynamics. However, much as in MCT, they also wrongly predict a *spurious* glass transition that is not at all present in actual systems, leading many people to dismiss these approaches altogether. In both cases the problem can be traced back to the mean-field (MF) nature of the approximations involved, and it has been argued that taking into account fluctuations beyond MF one can turn the spurious transition in the crossover observed in realistic systems [9, 10]. At any rate, while MF theory can be worked out analytically in full in the case of fully-connected Spin-Glasses models [11, 12] and supercooled liquids in the limit of infinite dimensions [13], *a mean-field theory of KCM was still lacking*. In this paper we solve this problem considering KCMs on the Bethe lattice (BL). Starting from some simple features of the dynamics as observed in actual numerical experiments we derive exact MCT-like dynamical equations in the most

straightforward way. This allows to easily compute the dynamical exponents and the predictions are then successfully validated by numerical simulations in a variety of models. We note that while the relevance of the field theoretical methods of Refs. [9, 10] in standard supercooled liquid models is still an open problem, one can consider specific models in physical dimension for which accurate quantitative predictions can be obtained in the regime where MF theory fails [14]. This requires the knowledge of various model-dependent constants, including MF dynamical exponents that in [14] could only be estimated from numerical simulation on the Bethe lattice. Thus the present work ensures that all the constants can be computed analytically, leading to fully *parameter-free* predictions, *i.e.* making the models solvable.

We consider the Fredrickson-Andersen (FA) KCM [7, 8]. Take a system of  $N$  independent Ising spins with Hamiltonian  $H = \beta/2 \sum_i s_i$ , meaning that an initial equilibrium configuration is easily generated numerically and that the density of negative spins is  $p = (1 + e^{-\beta})^{-1}$ . Complex behavior occurs because of a dynamic constraint: a spin can flip only if it has at least  $f$  (the facilitation) of its  $z$  nearest neighbors in the excited (up) state. The relevant observable is the persistence, that is equal to one until the spin flips for the first time and zero at all later times. Here following [14] we consider the persistence of the negative (blocking) spins. The FA model on the Bethe lattice is known to exhibit dynamical arrest [15–20]: at and below the critical temperature  $T_c$  the persistence converges to a plateau value  $\phi_{plat}$  that is approached in a power-law fashion. The FA dynamical transition is intimately related to bootstrap percolation (BP) and both  $T_c$  and  $\phi_{plat}$  can be computed from its solution on the Bethe lattice as we will recall later. In particular for connectivity  $z = 4$  and  $f = 2$  the average persistence  $\phi(t)$  obeys at  $T_c = 0.480898$  ( $p_c = 8/9$ ):

$$\phi(t) - \phi_{plat} \approx \frac{1}{(t/t_0)^a}, \quad t \gg 1, \quad (1)$$

where  $\phi_{plat} = 21/32$ . The problem is that through the mapping with BP we know the critical temperature and the plateau value (even their fluctuations [14, 21]), but *not* the dynamical exponent  $a$ . Furthermore numerical

simulations [14–16, 19] have shown that the transition has a Mode-Coupling-Theory nature, that amounts to a number of non-trivial features beyond the power-law decay at the critical temperature. In particular MCT behavior implies that for temperatures near  $T_c$  there is a  $\beta$ -regime corresponding to time-scales  $\tau_\beta$  on which the persistence is almost equal to  $\phi_{plat}$ . In the liquid phase ( $T > T_c$ ) this regime is followed by the  $\alpha$ -regime during which the persistence decays from  $\phi_{plat}$  to zero. In the  $\beta$ -regime the time-dependence of the persistence is controlled by the following scaling law [6]:

$$\phi(t) = \phi_{plat} + |\sigma|^{1/2} g_\pm(t/\tau_\beta) \quad (2)$$

where  $\sigma$  is a linear function of  $T_c - T$ , *i.e.* it is negative in the liquid phase ( $g_-(s)$  has to be used) and positive in the glassy phase ( $g_+(s)$  has to be used). The two scaling functions  $g_\pm(s)$  both diverge as  $1/s^a$  for small values of  $s$ , while for large values of  $s$   $g_+(s)$  goes to a constant, and  $g_-(s)$  diverges as  $-s^b$ . The model-dependent exponents  $a$  and  $b$  are determined by the so-called parameter exponent  $\lambda$  by:

$$\lambda = \frac{\Gamma^2(1-a)}{\Gamma(1-2a)} = \frac{\Gamma^2(1+b)}{\Gamma(1+2b)}. \quad (3)$$

The parameter exponent  $\lambda$  controls also the time scale of the  $\beta$  regime, that diverges with  $\sigma$  from both sides as  $\tau_\beta \propto |\sigma|^{-1/(2a)}$  with an unknown model-dependent factor. By using matching argument one can also argue that the time-scale of the  $\alpha$  regime increases as  $\tau_\alpha \propto |\sigma|^{-\gamma}$  with  $\gamma = 1/(2a) + 1/(2b)$ . Sellitto [16] has shown thoroughly that all the above non-trivial properties are satisfied in FA models on the BL as studied by means of numerical simulations: the problem is to understand why it is so and, if possible, to compute analytically the dynamical exponents. Following MCT, one can derive all the above properties under the *assumption* that  $g(t) \equiv \phi(t) - \phi_{plat}$  obeys the following quadratic equation [6] in the  $\beta$  regime:

$$\sigma = -\lambda g^2(t) + \frac{d}{dt} \int_0^t g(t')g(t-t')dt'. \quad (4)$$

In the following we show that the above equation indeed holds on the Bethe lattice, obtaining also analytical expression for the exponents  $a$  and  $b$  through the parameter  $\lambda$ . We present the argument considering the  $z = 4$ ,  $f = 2$  case at the critical probability  $p_c = 8/9$ . We then consider generic values of the facilitation and of the connectivity. This allow to demonstrate the theory more broadly including the case of continuous transitions where  $\phi_{plat} = 0$ . Successively we study models with random pinning [19], validating the theory in the context of a higher-order singularity characterized by logarithmic time decays. A further generalization considered is also the case of mixed facilitation [22].

To present the argument we need to introduce a number of definitions. The *blocked persistence*  $\phi_b(t)$  is the

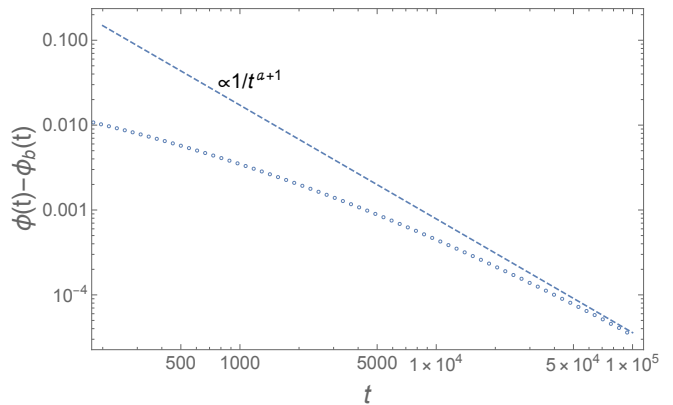


Figure 1. Difference between the average local persistence  $\phi(t)$  and  $\phi_b(t)$  (the average local persistence of the sites that have never been facilitated up to time  $t$ ) in the case of  $z = 4$  and  $f = 2$  at the critical temperature. The dashed line is the expectation  $C/t^{a+1} \propto d\phi/dt$ ,  $C \approx 180$ . The data correspond to the average of 80 samples of size  $N = 16 \times 10^6$ .

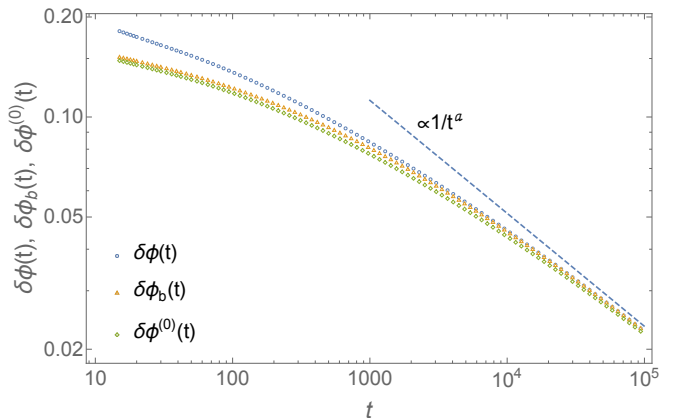


Figure 2. From bottom to top: zero-blocked persistence, blocked persistence, and persistence for  $z = 4$  and  $f = 2$  at the critical point. The data correspond to the average of 80 samples of size  $N = 16 \times 10^6$ .

fraction of negative spins that have been *blocked* at all times less than  $t$ . Naturally we have  $\phi(t) \geq \phi_b(t)$  as a spin that is facilitated (*i.e.* not blocked) does not necessarily flips, however one can argue that at large times  $\phi_b(t)$  and  $\phi(t)$  have the same critical behavior, *i.e.*  $\delta\phi_b(t) \equiv \phi_b(t) - \phi_{plat}$  and  $\delta\phi(t) \equiv \phi(t) - \phi_{plat}$  approach zero with the same leading term  $1/(t/t_0)^a$ . More precisely one can argue that the difference  $\phi(t) - \phi_b(t)$  is proportional to  $d\phi/dt$ , and thus it vanishes with a much faster power law  $1/t^{a+1}$ . We refer the reader to App. B for a complete discussion of this point. For now see Figs. 1 and 2 for a numerical confirmation of this expectation. We also define the *zero-switch blocked persistence*  $\phi_b^{(0)}(t)$  as the fraction of negative sites that have been blocked up to time  $t$  because at least three of their neighbors have remained in the negative state at all times less than  $t$ . The possible cases can be represented graph-

ically as:

$$\text{Diagram 1} + \text{Diagram 2} = \phi_b^{(0)}(t), \quad (5)$$

where the full lines represent the neighbors of the blocked site that have always remained negative. Finally we define the *one-switch blocked persistence*  $\phi_b^{(1)}(t)$  as the fraction of negative sites that have been blocked because two neighbors have been always negative, a third neighbor has been negative up to some  $t'$ , and a fourth neighbor has been negative between some time  $0 < t'' < t'$  and  $t$ . Note that this fourth neighbor should not have been negative at all times between 0 and  $t$ , since this contribution is already counted in  $\phi_b^{(0)}(t)$ . Again this can be represented graphically:

$$\text{Diagram 3} = \phi_b^{(1)}(t), \quad (6)$$

where the top left line represents the neighbor that is negative up to time  $t'$ , and the top right line represents the neighbor that is negative between  $t''$  and  $t$ . It is useful to clarify the origins of the names. At each time less than  $t$  a blocked site has a blocking set, *i.e.* a set of at least three neighbors in the negative (blocking) state: the *zero-switch* persistence count those spins for which at all times less than  $t$  the blocking set is the same, while the *one-switch* persistence counts those blocked spins for which the blocking set changes at time  $t'$ . Finally  $\Delta\phi_b(t) > 0$  counts all contributions to  $\phi_b(t)$  other than  $\phi_b^{(0)}(t)$  and  $\phi_b^{(1)}(t)$ :

$$\phi_b(t) = \phi_b^{(0)}(t) + \phi_b^{(1)}(t) + \Delta\phi_b(t). \quad (7)$$

The key observation is that at large times a *hierarchy* between the different contributions emerges, as shown in Fig. 3:

$$1 \gg \phi_b^{(0)}(t) - \phi_{plat} \gg \phi_b^{(1)}(t) \gg \Delta\phi_b(t) \quad t \gg 1. \quad (8)$$

Guided by these observations, in the following we will simply neglect  $\Delta\phi_b(t)$  at large times, obtaining a closed dynamical equation for the blocked persistence. Understanding the origin of this hierarchy is an interesting problem left for future work. The second inequality implies that the critical behavior of  $\phi_b(t)$  (and thus of  $\phi(t)$ ) is given by  $\phi_b^{(0)}(t)$  at leading order, as also shown by Fig. 2. In turn,  $\phi_b^{(0)}(t)$  can be written exactly in terms of the cavity persistence  $\hat{\phi}(t)$ , defined as the probability that a site persists in the negative state at all times smaller than  $t$  if we force one of its neighbors (the root) to be negative at all times. We have indeed:

$$\phi_b^{(0)}(t) = 4p \hat{\phi}(t)^3 (1 - \hat{\phi}(t)) + p \hat{\phi}(t)^4. \quad (9)$$

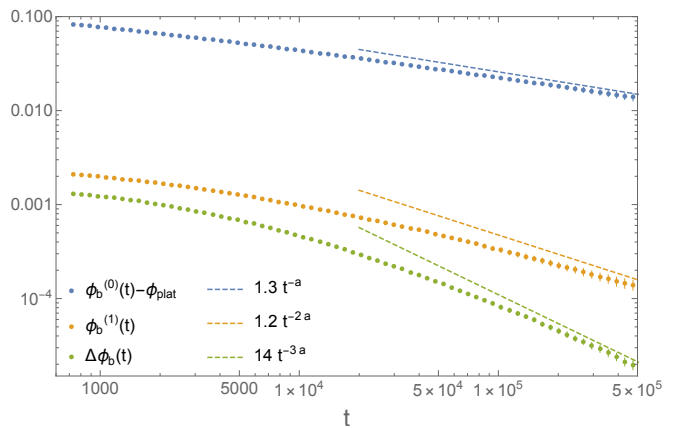


Figure 3. The hierarchy between the different contributions to the blocked persistence as observed in numerical simulations ( $N = 16 \times 10^6$ ).

The above equation is the same that one encounters in bootstrap percolation, and in particular at large times the distance from the plateau value is proportional to the difference between  $\hat{\phi}(t)$  and its plateau value  $\hat{\phi}_{plat} = 3/4$ . In particular at the critical temperature  $p_c = 8/9$  we have

$$\phi_b^{(0)}(t) - \phi_{plat} \approx \frac{3}{2} \delta\hat{\phi}(t), \quad \delta\hat{\phi}(t) \equiv \hat{\phi}(t) - \hat{\phi}_{plat}. \quad (10)$$

The cavity persistence is the typical object that occurs in analytical computations on the Bethe lattice, and indeed in the following we will show that it obeys a self-consistent equation. As we did for the persistence we introduce the blocked cavity persistence  $\hat{\phi}_b(t)$ , that counts the sites that were blocked at all times  $t' < t$ . Similarly to the site persistence one can argue that at large times  $\hat{\phi}_b(t)$  and  $\hat{\phi}(t)$  have the same critical behavior approaching  $\hat{\phi}_{plat}$  with the same leading term  $(2/3)/(t/t_0)^a$ . More precisely one can argue that the difference  $\hat{\phi}(t) - \hat{\phi}_b(t)$  is proportional to  $d\hat{\phi}/dt$  and thus it vanishes with a much faster power law  $1/t^{a+1}$ ,  $\hat{\phi}(t) = \hat{\phi}_b(t) + O(1/t^{a+1})$ . The cavity blocked persistence can be also written as a sum of zero-switch and one-switch terms:

$$\hat{\phi}_b(t) = \hat{\phi}_b^{(0)}(t) + \hat{\phi}_b^{(1)}(t) + \Delta\hat{\phi}_b(t), \quad (11)$$

and the crucial hierarchy emerges at large times as well:

$$1 \gg \hat{\phi}_b^{(0)}(t) - \hat{\phi}_{plat} \gg \hat{\phi}_b^{(1)}(t) \gg \Delta\hat{\phi}_b(t) \quad t \gg 1. \quad (12)$$

If we replace  $\delta\hat{\phi}_b(t)$  for  $\delta\hat{\phi}(t)$  (which is correct at order  $O(1/t^{a+1})$ ) and neglect  $\Delta\hat{\phi}_b(t)$  we obtain:

$$\delta\hat{\phi}(t) = \delta\hat{\phi}_b^{(0)}(t) + \hat{\phi}_b^{(1)}(t), \quad (13)$$

where both terms in the RHS can be expressed in terms of  $\delta\hat{\phi}(t)$  to obtain a closed equation. The zero-switch cavity persistence has exactly the the same expression of BP:

$$\hat{\phi}_b^{(0)}(t) = 3p \hat{\phi}(t)^2 (1 - \hat{\phi}(t)) + p \hat{\phi}(t)^3. \quad (14)$$

In particular, close to the critical temperature  $p_c = 8/9$ , *i.e.* for small  $\delta p \equiv p - p_c$ , we have at large times:

$$\delta\hat{\phi}_b^{(0)}(t) = \delta\hat{\phi}(t) + \frac{27}{32}\delta p - \frac{4}{3}\delta\hat{\phi}^2(t) + \dots \quad (15)$$

Note that the linear term  $\delta\hat{\phi}(t)$  cancels with the LHS of Eq. (13), and this is the reason why we have to study the equation at the next (quadratic) order, where  $\hat{\phi}_b^{(1)}(t)$  contributes. According to the definition of  $\hat{\phi}_b^{(1)}(t)$  we have one neighbor that remains negative up to a time  $t'$ , one neighbor that is negative between time  $t''$  and  $t$  with  $0 < t'' < t'$ , and a third neighbor that is negative at all times smaller than  $t$ . The probability that a cavity site flips between time  $t'$  and  $t' + dt'$  is given by  $-(d\hat{\phi}/dt')dt'$ . The total probability that one site is negative between time  $t''$  and  $t$  with  $0 < t'' < t'$  can be computed invoking the reversibility of the dynamics: it is equal to the probability that starting at equilibrium at time  $t$ , and moving backward in time the system is negative up to time  $t - t'$  but not up to time  $t$ , leading to a factor  $\hat{\phi}(t - t') - \hat{\phi}(t)$ . Integrating over  $t'$ , multiplying by a combinatorial factor counting all possible switching couples of neighbours, and multiplying by the probability  $\hat{\phi}(t)$  that the third neighbor remains negative at all times less than  $t$ , we obtain:

$$\hat{\phi}_b^{(1)}(t) = -6\hat{\phi}(t) \int_0^t \frac{d\hat{\phi}}{dt'} (\hat{\phi}(t - t') - \hat{\phi}(t)) dt' . \quad (16)$$

Therefore Eq. (13) evaluated at second order in  $\delta\hat{\phi}(t)$  becomes:

$$0 = \frac{27}{32}\delta p - \frac{4}{3}\delta\hat{\phi}^2(t) - \frac{9}{2} \int_0^t \frac{d\hat{\phi}}{dt'} (\hat{\phi}(t - t') - \hat{\phi}(t)) dt' , \quad (17)$$

which can be rewritten in the MCT form (Eq. (4)) with  $\sigma = 3/16\delta p$ , and

$$\lambda = \frac{2}{3} \rightarrow a = 0.340356, \quad b = 0.69661. \quad (18)$$

As we can see from Fig. 2, the predicted value compares well with the numerical data. A simple fit would yield a lower value of the exponent but a common error is to forget that power-laws typically have power-laws corrections. A safer procedure is to study the effective exponent  $a_{eff} \equiv -d \ln \delta\phi / d \ln t$  that converges to the actual exponent at large times. In Fig. 4 we plot parametrically the relative effective exponent  $(a_{eff} - a)/a$  as a function of  $\delta\phi(t)$ . A simple computation shows that if  $\delta\phi(t)$  can be written asymptotically as a sum of terms of order  $1/t^a$ ,  $1/t^{2a}$ ,  $1/t^{3a}$ , etc. the relative effective exponent converges to zero at small  $\delta\phi$  with corrections of order  $\delta\phi$ ,  $\delta\phi^2$ ,  $\delta\phi^3$  etc. From the figure we see that the effective exponent at the larger times reached by numerical simulations is still smaller than the predicted value by a few percent but it is definitively expected to grow at larger times. The dashed lines are guides for the eye interpolating between

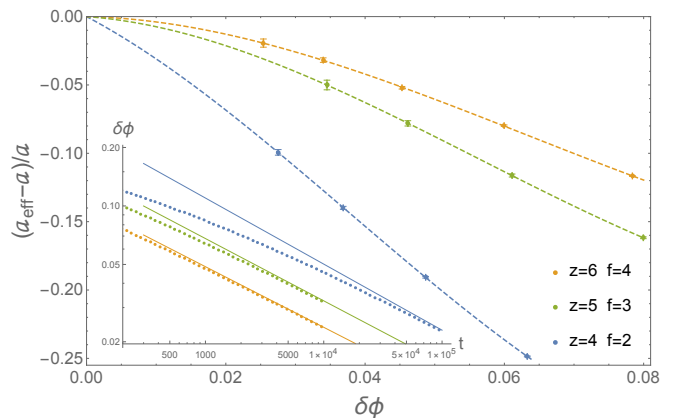


Figure 4. Relative shift of the effective exponent  $a_{eff}$  with respect to the analytical prediction  $a$ . From top to bottom (in the inset from bottom to top)  $z = 6$   $f = 4$ ,  $z = 5$   $f = 3$  and  $z = 4$   $f = 2$ . Each point is obtained by performing numerical simulations at different sizes ( $4 \times 10^6 \leq N \leq 32 \times 10^6$ ), and then extrapolating at infinite volume. The dashed lines are guides for the eye. Inset: distance of the persistence from the plateau value vs  $t$ . The continuous lines correspond to  $C_{z,f} t^{-a_{z,f}}$ , where the  $a_{z,f}$ 's are predicted analytically (see Table I), and  $C_{6,4} \approx 0.42$ ,  $C_{5,3} \approx 0.62$  and  $C_{4,2} \approx 1.15$ .

$z$	$f$	$p_c$	$\phi_{plat}$	$\lambda$	$a$	$b$
4	2	0.888889	0.65625	2/3	0.340356	0.69661
5	2	0.949219	0.855967	5/8	0.355765	0.768048
5	3	0.724842	0.413229	0.715095	0.32053	0.615707
6	2	0.970904	0.922852	3/5	0.364399	0.812034
6	3	0.834884	0.657417	0.690587	0.330849	0.656427
6	4	0.602788	0.294163	0.734359	0.311953	0.583922
7	2	0.981146	0.95232	7/12	0.369929	0.841922
7	3	0.88713	0.775028	0.672474	0.338095	0.686806
7	4	0.730978	0.522658	0.719926	0.318419	0.607721
7	5	0.513688	0.226228	0.744684	0.307169	0.566936

Table I. Dynamical parameters of the FA model on the Bethe lattice with connectivity  $z$  and facilitation  $f$ .

zero and the numerical data. Extracting more information from the numerical data is delicate, indeed simple extrapolations of the numerical results to  $\delta\phi = 0$  is not very safe as the series in  $\delta\phi$  is asymptotic because it contains powers of order  $O(\delta\phi^{1+1/a})$  corresponding to the terms  $1/t^{a+1}$  in  $\delta\phi(t)$ . The above computation can be generalized rather easily to the case of generic  $(z, f)$ . In table I we display the results up to  $z = 7$ , and the formulas are given in App. A. In Fig. 4 we plot the effective exponent for the (6, 4) and (5, 3) cases.

*Continuous Models* - For  $f = z - 1$  the BP transition occurs at  $p = 1/(z - 1)$  and it is continuous, that is  $\phi_{plat} = \hat{\phi}_{plat} = 0$ . One finds that for all values of the connectivity,  $\hat{\phi}(t)$  decays as  $t^{-a}$  with

$$\lambda = \frac{1}{2} \rightarrow a = 0.395263, \quad \forall z . \quad (19)$$

However at variance with the discontinuous case,  $\phi(t)$  is

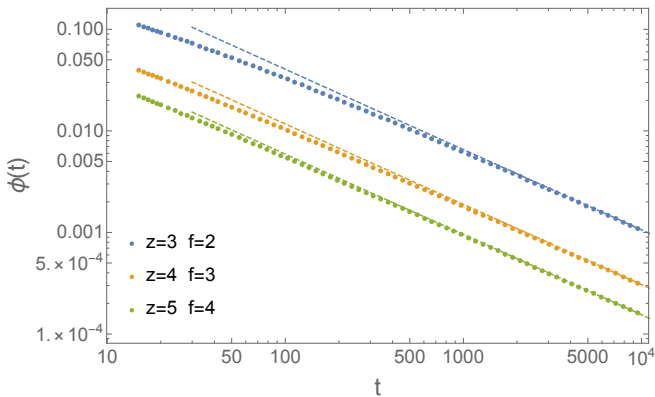


Figure 5. Persistence in continuous models,  $f = z - 1$ , for  $z = 3, 4, 5$ . The dashed lines correspond to  $C_z t^{-2a}$ , where  $a = 0.395263$  is the analytical prediction, and  $C_3 \approx 1.54$ ,  $C_4 \approx 0.45$  and  $C_5 \approx 0.23$ . Numerical data correspond to the average of 80 samples of size  $N = 16 \times 10^6$ .

quadratic in  $\hat{\phi}(t)$  and thus *its dynamic exponent is two times bigger*:

$$\phi(t) \approx \frac{z}{2} \hat{\phi}^2(t) \propto \frac{1}{t^{2a}}. \quad (20)$$

In Fig. 5 we show the persistence for connectivity three, four and five.

*A<sub>3</sub> singularity in random pinning* - In [19] it has been shown that random pinning allows to reach a higher-order critical point. In this case the dynamics has a further constraint: once the initial condition is generated with a given value of  $p$ , a fraction  $c$  of the spins is frozen and never updated. In the  $z = 4$ ,  $f = 2$  case, one finds a tricritical point at  $c = 1/5$  and  $p = 5/6$  with  $\phi_{plat} = 3/8$ , that is the end point of a line of discontinuous transitions in the  $(p, c)$  plane. At the tricritical point the transition becomes continuous, the parameter exponent takes the limiting value  $\lambda = 1$  (corresponding to  $a = 0$ ), and the decay becomes logarithmic. More precisely the deviation from the plateau value at the tricritical point is described asymptotically by the following equation:

$$0 = \mu g^3(t) - g^2(t) + \frac{d}{dt} \int_0^t g(t')g(t-t')dt'. \quad (21)$$

Equation (21) has been derived and studied in great detail by Götze and Sjögren [23]. Its solution yields a logarithmic decay of the  $g$ . More precisely at the leading and sub-leading order one has:

$$g(t) = \frac{4\zeta(2)}{\mu \ln^2(t/t_0)} + \frac{24\zeta(3)}{\mu \ln^3(t/t_0)} \ln \ln(t/t_0) + \dots \quad (22)$$

where  $\zeta(i)$  is the Riemann's  $\zeta$ -function and  $t_0$  is the unknown time scale that cannot be determined due to the time-scale invariance of equation (21). The dynamical computation in this case allows to determine the parameter  $\mu = 2/3$ . In Fig. 6 we plot the effective exponent

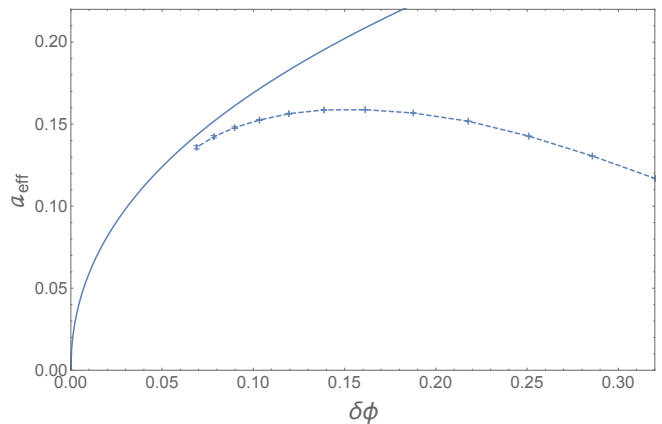


Figure 6. Effective exponent vs.  $\delta\phi$  at the  $A_3$  singularity of random pinning, see text. The continuous line is the prediction Eq. (22) with the analytically predicted value  $\mu = 2/3$ . Numerical data correspond to the average of 200 samples for  $N = 16 \times 10^6$ .

parametrically as a function of  $\delta\phi$ , together with the effective exponent corresponding to expression (22) with  $\mu = 2/3$ , as expected the effective exponent converges to zero at large times. The parametric expression allows to eliminate the dependence on the unknown timescale  $t_0$ .

*Mixed facilitation models* - Models with mixed facilitation display complex phase diagrams with higher-order singularities as well [22]. In particular we consider a  $z = 4$  Bethe lattice in which a fraction  $c$  of the spins has facilitation three, while the remaining  $1 - c$  fraction has facilitation two. In the  $(c, p)$  plane there is a line of continuous transition  $p_c = 1/(3c)$  from  $(1, 1/3)$  to the tricritical point  $(1/2, 2/3)$ . Along this line,  $\lambda = 1/(2c)$  changes from  $\lambda = 1/2$  to  $\lambda = 1$  at the tricritical point. On the line of discontinuous transition,  $p_c = (4(-2 + 3c))/(3(-3 + 4c))$ , that goes from the tricritical point  $(1/2, 2/3)$  to  $(0, 8/9)$ , we have instead:

$$\phi_{plat} = \frac{9(1 - 2c)^2(7 + 6c(-3 + 2c))}{4(-2 + 3c)^3(-3 + 4c)}, \quad \lambda = \frac{4 - 9c + 6c^2}{6 - 16c + 12c^2}.$$

In Fig. 7 we display numerical data for the persistence at  $c = 0.7, 0.8, 0.9, 1$ , together with the corresponding analytical predictions.

*Conclusions* - We have shown that the persistence of the FA model on the Bethe lattice obeys the critical equation of MCT. We note *en passant* that this provide one of the most simple derivations of this equation, the main ingredient being expression (16), which in turn is obtained by simple probabilistic arguments. The theory has been extended and validated in a variety of contexts. The possible extension to models with conserved dynamics, like the Kob-Andersen model [24–26] is left for future work.

It is remarkable that exact asymptotic equations can be obtained assuming that  $\Delta\phi_b(t)$  is negligible at large times (as suggested by numerical simulations) even without knowing the reason why. We are currently investigating this question, motivated also by the fact that the an-



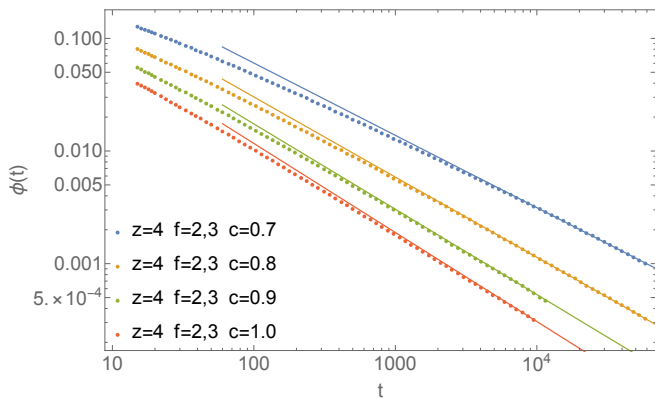


Figure 7. Persistence in models with mixed facilitation,  $f = 2, 3$   $z = 4$  for values of  $c = .7$  and  $c = .8$  corresponding to continuous transitions. The continuous lines correspond to  $C_c t^{-2a}$ , where  $a$  comes from the analytical prediction  $\lambda = (2c)^{-1}$  and  $C_{.7} \approx 1.16$ ,  $C_{.8} \approx 0.8$ ,  $C_{.9} \approx 0.57$ ,  $C_{1.0} \approx 0.45$ . Numerical data for  $N = 16 \times 10^6$ .

swer should eventually allow to compute systematically the corrections  $O(t^{-2a})$ ,  $O(t^{-3a})$ ,  $\dots$ , to the leading  $t^{-a}$  behavior. Note in particular that from Fig. 3,  $\Delta\phi_b(t)$  seems to decay as  $t^{-3a}$ . Another important motivation for a deeper understanding of the origin of the hierarchy is that in systems like spin-glasses and supercooled liquids in large dimensions the critical equation and the parameter exponent can be derived from the critical behavior of the overlap fluctuations [13, 27–30], whereas in the present case the overlap has regular fluctuations [18, 31] and therefore the mechanism underlying Eq. (4) in this case has to be totally different.

## ACKNOWLEDGMENTS

We acknowledge the financial support of the Simons Foundation (Grant No. 454949, Giorgio Parisi).

## APPENDIX

### A. The general case

The arguments of the (4, 2) case can be extended to generic  $(z, f)$  values. The critical probability and the plateau value can be expressed in terms of the function

$$F(P, k, f_b) \equiv \sum_{i=f_b}^k \binom{k}{i} P^i (1-P)^{k-1}. \quad (23)$$

The parameter  $P$  is the cavity value of the BP cluster, and obeys the equation:

$$P = p F(P, k, f_b), \quad (24)$$

where  $f_b \equiv k + 1 - f$  is the number of neighbors that must be blocked in the negative state (besides the root)

for the cavity site to be blocked in the negative state. At the critical temperature the above equation develops a solution with  $P \neq 0$ . In the discontinuous case  $P$  jumps from zero to a finite value at  $P_c$ . The finite value can be determined by the equation

$$\left( F(P_c, k, f_b) - P_c \left. \frac{dF(P, k, f_b)}{dP} \right|_{P=P_c} \right) P_c^{-f_b} = 0. \quad (25)$$

Note that the above equation is a polynomial of degree  $k - f_b$ , and thus the equation is linear for  $f = 2$ , and quadratic for  $f = 3$ . The critical probability is given by:

$$p_c = P_c / F(P_c, k, f_b), \quad (26)$$

while the plateau value is given by:

$$\phi_{plat} = p_c F(P_c, k + 1, f_b + 1). \quad (27)$$

The value of the parameter exponent is given by

$$\lambda = 1 + \frac{\frac{1}{2} \left. \frac{d^2 F(P, k, f_b)}{dP^2} \right|_{P=P_c}}{\binom{k}{f_b-1} (k - f_b + 1) (k - f_b) P_c^{f_b-1} (1 - P_c)^{k-f_b-1}}. \quad (28)$$

In particular for  $f = 2$  we have  $\lambda = \frac{1+k}{2k}$ .

### B. Difference between the persistence and the blocked persistence

For the sake of completeness let us now discuss why it is natural to expect that the critical behavior of  $\phi_b(t)$  is the same of  $\phi(t)$ . Let us note that in principle the spin could have been facilitated at some time in the past but did not switch due to a thermal fluctuation. However it is clear that the higher the number of times that it was facilitated, the lower the probability that it did not switch. Now due to the reversible nature of the dynamics, if the spin was facilitated at some distant time  $t'$  in the past with probability one, it must have been facilitated many times at later times, leading to a vanishing probability that it did not switch. In other words we expect that once a site becomes facilitated, it will switch with probability one after a finite time  $t_{sw}$  that is short on the time scale of the critical dynamics. The only possibility is that the site has become facilitated at a time  $t'$  close to  $t$ , *i.e.*  $t - t' = O(t_{sw})$ . On the other hand the number of sites that become facilitated between times  $t - t_{sw}$  and  $t$  is given by

$$\phi_b(t - t_{sw}) - \phi_b(t) \approx -t_{sw} \frac{d\phi_b(t)}{dt} \ll \phi_b(t), \quad (29)$$

thus we expect that the difference between  $\phi(t)$  and  $\phi_b(t)$  is proportional  $O(1/t^{a+1})$  at large times, and that it can be neglected with respect to  $1/t^a$ . The argument is confirmed by the numerical data (see Fig. 1).

- 
- [1] G. Biroli and J. P. Garrahan, *The Journal of chemical physics* **138**, 12A301 (2013).
- [2] F. Ritort and P. Sollich, *Advances in physics* **52**, 219 (2003).
- [3] J. P. Garrahan, P. Sollich, and C. Toninelli, *Dynamical heterogeneities in glasses, colloids, and granular media* **150**, 111 (2011).
- [4] B. Guiselin, C. Scalliet, and L. Berthier, *Nature Physics* **18**, 468 (2022).
- [5] A. S. Keys, L. O. Hedges, J. P. Garrahan, S. C. Glotzer, and D. Chandler, *Physical Review X* **1**, 021013 (2011).
- [6] W. Götze, *Complex dynamics of glass-forming liquids: A mode-coupling theory*, Vol. 143 (OUP Oxford, 2008).
- [7] G. H. Fredrickson and H. C. Andersen, *Phys. Rev. Lett.* **53**, 1244 (1984).
- [8] G. H. Fredrickson and H. C. Andersen, *J. Chem. Phys.* **83**, 5822 (1985).
- [9] T. Rizzo, *EPL (Europhysics Letters)* **106**, 56003 (2014).
- [10] T. Rizzo, *Phys. Rev. B* **94**, 014202 (2016).
- [11] M. Mézard, G. Parisi, and M. A. Virasoro, *Spin glass theory and beyond: An Introduction to the Replica Method and Its Applications*, Vol. 9 (World Scientific Publishing Company, 1987).
- [12] T. Castellani and A. Cavagna, *Journal of Statistical Mechanics: Theory and Experiment* **2005**, P05012 (2005).
- [13] G. Parisi, P. Urbani, and F. Zamponi, *Theory of simple glasses: exact solutions in infinite dimensions* (Cambridge University Press, 2020).
- [14] T. Rizzo and T. Voigtmann, *Physical Review Letters* **124**, 195501 (2020).
- [15] M. Sellitto, G. Biroli, and C. Toninelli, *EPL (Europhysics Letters)* **69**, 496 (2005).
- [16] M. Sellitto, *Phys. Rev. Lett.* **115**, 225701 (2015).
- [17] A. De Candia, A. Fierro, and A. Coniglio, *Sci. Rep.* **6**, 26481 (2016).
- [18] S. Franz and M. Sellitto, *JSTAT* **2013** (02), P02025.
- [19] H. Ikeda, K. Miyazaki, and G. Biroli, *EPL (Europhysics Letters)* **116**, 56004 (2017).
- [20] F. Sausset, C. Toninelli, G. Biroli, and G. Tarjus, *J. Stat. Phys.* **138**, 411 (2010).
- [21] T. Rizzo, *Phys. Rev. Lett.* **122**, 108301 (2019).
- [22] M. Sellitto, D. De Martino, F. Caccioli, and J. J. Arenzon, *Physical review letters* **105**, 265704 (2010).
- [23] W. Götze and L. Sjögren, *Journal of Physics: Condensed Matter* **1**, 4203 (1989).
- [24] W. Kob and H. C. Andersen, *Physical Review E* **48**, 4364 (1993).
- [25] C. Toninelli, G. Biroli, and D. S. Fisher, *Journal of statistical physics* **120**, 167 (2005).
- [26] R. Boccagna, *The European Physical Journal Special Topics* **226**, 2311 (2017).
- [27] F. Caltagirone, U. Ferrari, L. Leuzzi, G. Parisi, F. Ricci-Tersenghi, and T. Rizzo, *Phys. Rev. Lett.* **108**, 085702 (2012).
- [28] G. Parisi and T. Rizzo, *Phys. Rev. E* **87**, 012101 (2013).
- [29] G. Parisi, F. Ricci-Tersenghi, and T. Rizzo, *JSTAT* **2014** (4), P04013.
- [30] T. Rizzo, *Stochastic equations and dynamics beyond mean-field theory*, in *Spin Glass Theory and Far Beyond: Replica Symmetry Breaking After 40 Years*, edited by P. Charbonneau, E. Marinari, M. Mézard, G. Parisi, F. Ricci-Tersenghi, G. Sicuro, and F. Zamponi (Singapore: World Scientific, 2023).
- [31] G. Perrupato and T. Rizzo, In preparation.